Atmos. Chem. Phys. Discuss., 12, 7677–7704, 2012
www.atmos-chem-phys-discuss.net/12/7677/2012/
doi:10.5194/acpd-12-7677-2012

Atmospheric Chemistry and Physics Discussions

Eddy covariance measurements of CO_2 and energy fluxes in the city of Beijing

H. Z. Liu[1], J. W. Feng[1], L. Järvi[2], and T. Vesala[2]

[1]LAPC, Institute of Atmospheric Physics, Chinese Academy of Sciences, Beijing 100029, China
[2]Department of Physics, University of Helsinki, P.O. Box 48, 00014 University of Helsinki, Finland

Received: 25 November 2011 – Accepted: 6 February 2012 – Published: 16 March 2012

Correspondence to: H. Z. Liu (huizhil@mail.iap.ac.cn)

Published by Copernicus Publications on behalf of the European Geosciences Union.

Abstract

Long-term measurement of carbon dioxide flux (F_c) was performed using the eddy covariance (EC) method in the Beijing megacity over a 4-yr period in 2006–2009. The EC setup was installed at a height of 47 m on the Beijing 325-m meteorological tower in the northwest part of the city. Latent heat flux dominated the energy exchange between the urban surface and the atmosphere in summer, while sensible heat flux was the main component in the spring. The source area of the measurements of CO_2 is highly heterogeneous, which consists of buildings, parks, and highways. It is valuable for global carbon budget research to study the temporal and spatial variability of F_c in this urban environment of a developing country. Both on a diurnal and monthly scale, the urban surface acted as a net source for CO_2 and downward fluxes were only occasionally observed. The diurnal pattern of F_c showed dependence on automobile traffic and the typical two peak traffic pattern appeared in F_c diurnal cycle. Also, the F_c was higher on weekdays than on weekends due to the higher traffic volumes on weekdays. On seasonal scale, F_c was generally higher in winter than during other seasons, likely due to domestic heating during colder months. Total annual average CO_2 emissions were estimated to be 4.90 $kg\,C\,m^{-2}\,y^{-1}$ over the 4-yr period.

1 Introduction

The proportion of the world's population living in urban areas has increased over the past several decades. In China, urbanization has rapidly increased following the reform and opening policy in effect since 1978. At the end of 2009, 46.6 % (about 622 million) of China's inhabitants resided in urban environments and this fraction is expected to increase (Pan and Niu, 2010). One of the most important impacts of urbanization on local and regional climates is the emissions of greenhouse gases (primarily CO_2) to the atmosphere and changes in land use (Kalnay and Cai, 2003). Urban areas emit 30–40 % of all anthropogenic greenhouse gases, even though they currently cover only about 4 % of the world's dry land surface (Satterthwaite, 2008). CO_2 is one of the most important greenhouse gases, and a significant increase in CO_2 concentrations from 280 ppm in pre-industrial times to 379 ppm in 2005 is the probable cause of the mean air temperature increase of approximately 0.6 °C observed during the last 100 yr (IPCC AR4, 2007). However, knowledge of the magnitude and temporal variability of surface-atmosphere CO_2 exchange in cities has been limited up until the recent years. There is a need to make continuous CO_2 exchange measurements over urban surfaces to provide useful information for CO_2 emission monitoring and to local policy- and decision-makers to make plans to reduce CO_2 emissions from anthropogenic sources.

Quantification of the urban CO_2 emissions is difficult due to the complex morphological nature of the urban landscape. The most common approaches to quantifying urban CO_2 emission are based on estimates of fossil fuel consumption rather than direct measurements of CO_2 concentration or flux (Grimmond et al., 2002; Vogt et al., 2006). These approaches do not, however, consider the heterogeneity and variability of the emission sources (Velasco and Roth, 2010). Advances in instrumentation, notably the eddy covariance (EC) technique, offer a tool to directly measure representative flux data from urban areas. The EC technique has been widely used to measure the net CO_2 exchange of various natural or agricultural ecosystems as part of the global flux network (Baldocchi et al., 2000, 2001), but its application in urban areas remains less common. With a few exceptions (Crawford et al., 2011), existing, published long-term (>3 yr) urban flux data sets are rare. Moreover, urban EC studies have mainly focused on cities in developed countries (e.g. Bergeron and Strachan, 2011; Coutts et al., 2007; Grimmond et al., 2002; Matese et al., 2009; Nemitz et al., 2002; Pawlak et al., 2011; Vesala et al., 2008; Vogt et al., 2006). The characteristics of urban CO_2 exchange in developing countries, where the degree of industrialization is relatively lower than that in developed countries, are largely unknown, with the only reported measurements from Mexico City (Velasco et al., 2009) and Cairo (Burri et al., 2009).

Urban CO_2 exchange measured with the EC method represent an integrated response from anthropogenic, biogenic and meteorological factors, and the distribution of their sources and sinks is highly heterogeneous (Vogt et al., 2006). However, urban areas are consistently reported to be a net source for CO_2 on both daily and seasonal timescales, with a strong dependence on the vegetation fraction and human activities (Coutts et al., 2007; Grimmond et al., 2002, 2004; Helfter et al., 2011; Matese et al., 2009; Velasco et al., 2009; Vesala et al., 2008; Vogt et al., 2006). Maximum emissions are typically observed to be consistent with the highest traffic volumes during rush hours (Coutts et al., 2007; Vesala et al., 2008). Previous studies have also shown large variations of CO_2 flux on seasonal timescales (Bergeron and Strachan, 2011; Crawford et al., 2011; Pawlak et al., 2011; Vesala et al., 2008). Besides traffic, fossil fuel burning for domestic heating can also cause high CO_2 emission levels in winter (Bergeron and Strachan, 2011; Matese et al., 2009; Pawlak et al., 2011). In dense urban areas, CO_2 flux is partly reduced by urban vegetation in summer, but the effect is not typically significant enough to offset the emissions from anthropogenic sources (Coutts et al., 2007; Grimmond et al., 2002).

As part of its promise to stage a green Olympics in 2008, Beijing made great efforts to improve its air quality. An odd-even traffic restriction scheme was implemented to reduce traffic congestion on the roads for two months (from July 20 to September 20). On days when odd numbered license plates were allowed, vehicles with license plates ending in an even number were prohibited from operating. This regulation was expected to take 45 percent of the city's 3.29 million vehicles off the roads and to reduce vehicle emissions by 63 %. In addition, many factories both in and around Beijing were closed for the duration of the Games because they were not expected to meet the temporarily increased environmental standards. Song and Wang (2012) analyzed the impact of the reduction of vehicles on CO_2 flux during the Games, and found significant lower flux during this period. However, the analysis was restricted to a year. The differences of CO_2 flux between weekdays and weekends, and the annual variations of CO_2 emission in the long-term are of interest.

ACPD
12, 7677–7704, 2012

This study shows the first long-term urban CO_2 flux (F_c) from Beijing megacity measured with the EC method. This article also contributes to the small number of studies on the net CO_2 exchange in developing countries. The objectives of this study are: (1) to quantify the magnitude of F_c in Beijing; (2) to examine the temporal F_c patterns at diurnal, seasonal, and annual time scales; (3) to examine the spatial variability of F_c in a complex urban environment; and (4) to examine the annual variations of total CO_2 emission.

2 Site description and instrumentation

2.1 The Beijing megacity

Beijing, the capital of China, is among the most developed cities in China. It is located in the northern part of the North China Plain and is surrounded by the Yanshan Mountains to the west, north, and east, whereas the small alluvial plain of the Yongding River lies to its southeast. The city has a moderate continental climate with hot, humid summers due to the East Asian monsoon and winters that are generally cold and dry, reflecting the influence of the Siberian anticyclone. The total population in Beijing exceeded 22 million at the end of 2009, making it one of the largest megacities in the world. The municipality's area was estimated to be 16 800 km^2 and the population density 1309 people per km^2 in 2009. Caused by rapid urbanization, the increase in vehicle numbers in Beijing has been dramatic: the number of registered vehicles has increased from 2.9 million in 2006 to 4 million by the end of 2009.

2.2 Site description

The measurements were carried out at a 325-m meteorological tower (39°58′ N, 116°22′ E, 60 m a.s.l.) in the northwest part of Beijing, about 8 km from Tiananmen Square. The tower, built in 1979, has specially been designed for meteorological observation and environmental monitoring. At the time when the tower was built, the surrounding area was a less built-up area covered by rural croplands and could be classified as suburban. As a result of the rapid urbanization of Beijing since 1980s, the surroundings of the tower have been totally altered to be an urban area and are nowadays clearly more heterogeneous (Fig. 1). The tower adjoins a small park of about 0.3 km^2 in the west mainly consisting of deciduous trees and lawns. To the east of the tower, an expressway (the Beijing-Tibet Expressway) with heavy traffic loads crosses from south to north. Another busy road (Beitucheng West Road) crossing from east to west is located north of the tower. Dense residential buildings are situated in the south and the north, and these areas are characterized by low vegetation cover. The percentage of vegetated area within a circle around the tower corresponding to about 90 % of the footprints, as derived from satellite photographs via color filtering techniques, is approximately 15 %. Within a circle corresponding to 50 % of the footprints, the surrounding area can be divided into four surface cover sectors: the NE sector and the SE sector can be classified as "compact midrise", the SW sector as "compact highrise" and the NW sector as "close-set trees" according to the classification system proposed by Stewart (2009). According to the estimations using the wind profile obsersvations from the tower by Li et al. (2003), the aerodynamic roughness lengths (z_0) in NE, SE, SW, and NW are 2.5 m, 3.0 m, 5.3 m, and 2.8 m, respectively, and the zero-plane displacement heights (d) are 12.3 m, 15.0 m, 26.4 m, and 13.2 m, respectively. The larger z_0 and d in the southwest can be attributed to the tall residential buildings (with the mean height of 45.0 m) in this direction. The vegetation fractions for the four sectors are estimated to be 10.7 %, 18.2 %, 12.9 % and 18.6 %, respectively.

2.3 Instrumentation

The EC setup was mounted 47 m above the ground to continuously measure the exchange of CO_2, heat, water, and momentum. The measurement height is almost 3 times the mean displacement height (~16.7 m) in the close surroundings (except in the SW sector), which ensured that measurements were taken in the constant flux layer (Grimmond et al., 2002). The EC setup was mounted on a 2-m horizontal boom

ACPD
12, 7677–7704, 2012

to minimize flow distortions from the tower. A three-dimensional sonic anemometer (CSAT3, Campbell Scientific Inc., Logan, Utah, USA) was used to directly measure horizontal and vertical wind velocity components and virtual temperature. An open-path infrared gas analyzer (IRGA, LI-7500, Licor Inc., Lincoln, NE, USA) was used to measure fluctuations of water vapor and CO_2 concentrations. Both instruments were operated at a sampling frequency of 10 Hz. The IRGA was calibrated at an interval of six months using a dew point generator and standard gases. In addition, air temperature and humidity at the same level were measured using a thermometer and a hygrometer (developed in Institute of Atmospheric Physics). In addition, wind speed and direction were measured at 15 different levels (8 m, 15 m, 32 m, 47 m, 63 m, 80 m, 102 m, 120 m, 140 m, 160 m, 180 m, 200 m, 240 m, 280 m, 320 m) using cup anemometers and vanes (developed in Institute of Atmospheric Physics). The daily and monthly precipitation or air temperature data were obtained from the Caoyang weather station about 10 km southeast of the site.

3 Method

In this study we analyzed the EC data over four-year period from 2006 to 2009. Vertical flux F was calculated as a covariance between the vertical velocity w and scalar s of interest according to the eddy covariance technique (Lee et al., 2004):

$$F = \overline{w's'} \tag{1}$$

Before calculating half-hourly fluxes of CO_2, water, sensible heat and momentum, spike detection and data rejection algorithms were applied using dynamic mean and standard deviation values within a series of moving windows as described by Vickers and Mahrt (1997). Data were rotated into streamwise coordinate system using a double rotation procedure so that the mean vertical velocity was forced to be zero (Kaimal and Finnigan, 1994). The sonic temperature for humidity was corrected following Schotanus et al. (1983). Theoretical spectral corrections (about 2 % of the original

ACPD
12, 7677–7704, 2012

fluxes) were made for high-frequency losses due to sensor separations, path averaging and sensor frequency response (Massman and Lee, 2002). The water vapor and CO_2 fluxes were also corrected for the density fluctuations (Webb et al., 1980). Data quality was assessed using the steady state test and integral turbulence characteristic test suggested by Foken et al. (2004). Data not passing the tests were excluded from the analysis. It should be noted that nocturnal fluxes in non-urban ecosystems are known to be underestimated by EC measurements due to the low-turbulence conditions prevailing at night (Aubinet, 2008). However, the u_* filtering approach is problematic in urban areas because the urban boundary layer is not always stable at night due to anthropogenic heat emissions, releases of storage heat to the boundary layer, and the heterogeneity of the urban canopy (Crawford et al., 2011). Therefore, no u_* filtering was applied in this study.

Data gaps originating from power failures, instrument calibration errors, and sensor malfunctions accounted for 13.2 % during the four-year study period. Out-of-range data removal and spikes detection (outside 3 times of standard deviation from mean value) removed an extra 3.1 % of data. Low-quality data caused by precipitation, dust, or other contamination on the sensor optics, which were indicated by the active gain control (AGC) values of the LI-7500, resulted in 6.9 % of eliminated data. Data that failed the stationary test caused another 6.1 % of the data gaps. Overall, the data coverage for the study period was approximately 70 %. Missing data were reconstructed using a gap-filling strategy as follows: (1) small gaps (<2 h) were replaced with linear interpolations; (2) medium gaps (<2 days) were rebuilt based on the mean diurnal variation (MDV) on adjacent days (Falge et al., 2001); and (3) large gaps (>2 days) were rebuilt using a multiple imputation method following Hui et al. (2003). Related meteorological variables such as air temperature, humidity, and wind direction were input in the imputation.

ACPD
12, 7677–7704, 2012

4 Results and discussion

4.1 Environmental conditions

General meteorological conditions during the study period are shown in Fig. 2. The annual total precipitation in Beijing for the four-year period was 473 mm in 2006, 452 mm in 2007, 619 mm in 2008, and 606 mm in 2009, respectively, with maxima observed during the summer months. The average air temperature over the 4-yr period was 13.3 °C and the extreme air temperatures during the study period ranged from −14.6 °C in February to 37.7 °C in June. The hot and rainy summers are caused by the monsoon winds that bring warm and humid air from the southeast to the Beijing area. Observations of the atmospheric stability defined as $\zeta = (z - d)/L$, where z is the measurement height and L is the Obukhov length, showed that the number of unstable cases ($\zeta < -0.05$) was about 10 % more than the number of stable cases (Fig. 3a). Also 8.6 % of the unstable cases were observed to occur during nighttime (Fig. 3b). The fraction of unstable cases in Beijing is much lower than observed in London where unstable cases were three times more common than stable cases (Wood et al., 2010). Also, the number of unstable half hour periods at nighttime was much higher in London than in this study indicating higher nocturnal heat emissions to the atmosphere in their source area. The wind rose measured over the 4-yr period showed prevailing northwesterly and southeasterly winds (Fig. 4). Winds from the 270 °–360 ° sector occurred during 39.5 % of the study period, whereas the 90°–180° sector accounted for 33.9 % of the study period. It should be noted that high wind speeds were recorded more frequently in the northwest sector, whereas the southwest sector experienced low wind speeds due to the tall buildings in this direction.

4.2 Time series of turbulence fluxes

Figure 5 shows the annual behavior of sensible heat flux (H), latent heat flux (Le), and carbon dioxide flux (F_c) at 30-min intervals, and the daily precipitation measured at Caoyang weather station. Also, monthly Bowen ratio calculated as a ratio between the sensible heat and latent heat fluxes is plotted. During the dry seasons, H is the dominant heat flux and reaches its maximum of 250–300 $W\,m^{-2}$ in spring. Le is small (generally less than 100 $W\,m^{-2}$) during the dry season due to the lack of precipitation and therefore also evaporation (Fig. 5e). Bowen ratio reaches its maximum 2–2.5 just in the beginning of the dry season when Le is below 100 $W\,m^{-2}$. During the rainy season, Le reaches its maximum of 250–350 $W\,m^{-2}$ in July or August, and the Bowen ratio decreases to less than 0.5 (Fig. 5d). Positive (upward) F_c ranging between 0–3 $mg\,m^{-2}\,s^{-1}$ are observed regardless of the season, while negative (downward) F_c are only observed occasionally, with values generally from −1.5 to 0 $mg\,m^{-2}\,s^{-1}$ (Fig. 5c). This indicates that CO_2 emissions dominate the CO_2 exchange between the urban surface and the atmosphere. Furthermore, the largest upward fluxes are observed in winter during the colder months when likely more traffic and domestic heating take place. The characteristic features of F_c variability on diurnal, seasonal and annual time scales analyzed below are based on this time series.

4.3 Diurnal variation of energy fluxes

Average course of Le was found to be significantly changed between summer and winter (Fig. 6). Maximum Le at midday was observed to be 137.1 $W\,m^{-2}$ in JJA, while it was less than 20 $W\,m^{-2}$ in DJF. The much higher Le in summer was caused by the large amount of precipitation brought by the monsoon. Maximum H at midday was observed to be 67.8 $W\,m^{-2}$ in JJA, while it was 82.1 $W\,m^{-2}$ in DJF. The difference in the average course of H between summer and winter was not significant, with slightly higher maximum values at midday in winter. The results indicate that the climate makes a clear distinction between the wet and dry season in Beijing city. The relationship between energy fluxes and climate in urban areas is beyond the scope of this paper and will not be discussed here.

ACPD
12, 7677–7704, 2012

4.4 Diurnal variation of F_c

For the diurnal F_c patterns, data were averaged over seasons (winter = DJF, spring = MAM, summer = JJA and fall = SON) due to similarities in months (Fig. 7). During all seasons the nocturnal fluxes are lower than in daytime when the diurnal variation is characterized by a distinct two peak pattern following the traffic rush hours. In winter, higher F_c is measured over the mean diurnal course, ranging from 15.9 to 31.82 $\mu mol\,m^{-2}\,s^{-1}$, with an average value of 18.86 $\mu mol\,m^{-2}\,s^{-1}$. Also, the morning peak is pronounced in winter, likely due to increased emissions from fossil fuel usage during the colder months. Also, the morning peak seemed to have two maxima: the first 26.59 $\mu mol\,m^{-2}\,s^{-1}$ appeared at 08:00 and is related to intensive traffic flow. The second peak 30.45 $mg\,m^{-2}\,s^{-1}$ at 11:00 is likely caused by human activity and the more unstable stratification during daytime (Fig. 3b). On some occasions during the study period, the morning peak reached 68.18 $\mu mol\,m^{-2}\,s^{-1}$. During other seasons, the net CO_2 fluxes are lower due to the increase in biological processes and reduction in anthropogenic emissions. In summer, the mean diurnal course ranged from 8.86 to 18.86 $\mu mol\,m^{-2}\,s^{-1}$, with an average of 12.73 $\mu mol\,m^{-2}\,s^{-1}$. Unlike in winter, the morning peak of F_c has a flat maximum, as human activities began earlier during the warm season and there is an earlier sunrise. In all seasons the evening peak is broad and maxima are observed between 18:00–20:00, indicating emissions from cooking and other household activity after returning from work. In summer, the peak extended longer due to the longer day. The consistently positive values of F_c indicate that the source area is always a net source of CO_2.

As automobile traffic is a considerable source of CO_2, the diurnal variations were also analyzed independently for weekdays and weekends (Fig. 7). F_c in weekdays and weekends are very similar through the year, except during the morning rush hours when higher emissions are observed during the weekdays. This is due to the vehicular traffic caused by the work commuters. It seems that in Beijing the difference between weekday and weekend traffic is not as pronounced as is typically observed in cities

ACPD
12, 7677–7704, 2012

in Western countries. Otherwise, the observed diurnal behavior of F_c follows those measured in other cities where pronounced two peaked pattern has been observed (Coutts et al., 2007; Bergeron and Strachan, 2011; Vesala et al., 2008; Vogt et al., 2006). The mean values of F_c measured at our site (18.86 µmol m^{-2} s^{-1}) in winter are lower than those in Montreal, Canada (~20.0 µmol m^{-2} s^{-1}) (Bergeron and Strachan, 2011) and Firenze, Italy (~25.68 µmol m^{-2} s^{-1}) (Matese et al., 2009). The mean values of F_c measured in the summer at our site were, by contrast, higher than those recorded in Mexico City in Mexico (~9.32 µmol m^{-2} s^{-1}) (Velasco et al., 2009), Melbourne in Australia (~10.91 µmol m^{-2} s^{-1}) (Coutts et al., 2007), and Basel in Switzerland (~12.5 µmol m^{-2} s^{-1}) (Vogt et al., 2006).

4.5 Spatial variation of F_c

The net CO_2 exchange between the atmosphere and the urban surface is a result of a combination of anthropogenic and biogenic processes. CO_2 sources and sinks are heterogeneous within the flux source area. By analyzing the differences in F_c values based on wind direction, it is possible to investigate the role of local sources in different surface cover areas (Fig. 8).

In winter, the dominant wind direction is northwest with 49 % of airflows coming from this direction. The highest F_c values, i.e., about 28.41 µmol m^{-2} s^{-1} during the daytime, are observed from the northeast portion of the study area, which corresponds to the sector with the heaviest traffic loads. During the night, F_c values in the east and northeast are substantially reduced due to the reduction of automobile traffic. On cold winter nights, people usually do not go outside, and automobile traffic volumes are much lower than usual. The highest F_c values were measured when winds blow from the northwest and south, where two dense residential areas are situated.

In summer, the heavy automobile traffic on the expressway and the prevalent southeasterly winds contributed to the highest daytime F_c values (about 22.73 µmol m^{-2} s^{-1}). The measured F_c values in the west were much lower due to CO_2 uptake by vegetation

ACPD
12, 7677–7704, 2012

in the park. The photosynthetic processes by urban vegetation, even in such a small park, can play a role in the absorption of CO_2. At night, F_c generally drops below 9.10 µmol m^{-2} s^{-1}, except in the southeast. The higher F_c values in the southeast are due to CO_2 emissions from the expressway in the prevalent wind direction. The results reveal that F_c in urban areas is largely determined by the prevailing surface cover within the flux source area.

4.6 Annual variability of F_c

Seasonal and annual variations of F_c were assessed by calculating average monthly F_c from the non-gap-filled half hourly dataset. As already shown by the diurnal behavior of F_c, the average monthly F_c is always positive regardless of the month (Fig. 9). The annual variation of F_c is characterized by an annual time course that varies inversely with air temperature. A negative correlation between the average monthly F_c and average monthly air temperature is observed (Fig. 10), which is the combined effect of fuel combustion and vegetation uptake. With all gaps filled, the urban surface is a net source of carbon dioxide annually, with an average of 4.90 kg C m^{-2} y^{-1} released to the atmosphere. Annual CO_2 emissions for this site are estimated as 4.77 kg C m^{-2} y^{-1} in 2006, 4.80 kg C m^{-2} y^{-1} in 2007, 4.61 kg C m^{-2} y^{-1} in 2008, and 5.40 kg CO_2 m^{-2} y^{-1} in 2009. The higher CO_2 emission in 2009 is possibly due to the reopening of some factories after the Olympic Games and more production made up for the cessation. Our results are within the range of other annual totals reported in the literature (Table 1).

5 Conclusions

This article presents the first result of direct CO_2 flux measurement in the city of Beijing. CO_2 flux was measured for a period of 4 yr in the northwest part of the city to assess the temporal variations from the diurnal to the annual scale. Based on the measurements, the results from this study permit the following conclusions: (1) Diurnal time courses

ACPD
12, 7677–7704, 2012

of CO_2 flux largely depend on automobile traffic. The two peaks in the morning and the evening correspond to the highest traffic volumes of the day. The daytime CO_2 flux is partly moderated by urban vegetation in the warm season. (2) The consistently positive CO_2 flux throughout the year indicates that the analyzed urban surface is a net source of CO_2 to the atmosphere. Emissions from domestic heating are a considerable source of CO_2 in the winter. CO_2 sequestration by urban vegetation is not sufficient to offset emissions from local sources. (3) Spatial variation patterns of CO_2 flux are mainly determined by the prevailing surface cover within the flux source area. (4) The integrated annual net CO_2 exchange over the 4-yr period calculated from a gap-filled F_c dataset is 4.90 kg C m^{-2} y^{-1}. This study shows an application of the eddy covariance technique to long-term monitoring of CO_2 flux in a densely built urban area. The results presented here can provide valuable information for urban development and help to shape policies for the reduction of greenhouse gases emissions.

Acknowledgements. This research was supported by NSFC projects (41030106, 41021004), and the National Basic Research Program of China (973 Program, 2010CB951801). The authors thank Senior Engineer Li Aiguo (LAPC/IAP, CAS) for maintaining the observation system.

References

Aubinet, M.: Eddy covariance CO_2 flux measurements in nocturnal conditions: An analysis of the problem, Ecol. Appl., 18, 1368–1378, 2008.

Baldocchi, D., Finnigan, J., Wilson, K., Paw U, K. T., and Falge, E.: On measuring net ecosystem carbon exchange over tall vegetation on complex terrain, Bound-Lay. Meteorol., 96, 257–291, 2000.

Baldocchi, D., Falge, E., Gu, L., Olson, R., Hollinger, D., Running, S., Anthoni, P., Bernhofer, C., Davis, K., and Evans, R.: FLUXNET: A new tool to study the temporal and spatial variability of ecosystem-scale carbon dioxide, water vapor, and energy flux densities, B. Am. Meteorol. Soc., 82, 2415–2434, 2001.

Bergeron, O. and Strachan, I. B.: CO_2 sources and sinks in urban and suburban areas of a northern mid-latitude city, Atmos. Environ., 45, 1564–1573, 2011.

ACPD

12, 7677–7704, 2012

Burri, S., Frey, C., Parlow, E., and Vogt, R.: CO_2 fluxes and concentrations over an urban surface in Cairo/Egypt, The seventh International Conference on Urban Climate, Yokohama, Japan, 2009.

Coutts, A. M., Beringer, J., and Tapper, N. J.: Characteristics influencing the variability of urban CO_2 fluxes in Melbourne, Australia, Atmos. Environ., 41, 51–62, 2007.

Crawford, B., Grimmond, C. S. B., and Christen, A.: Five years of carbon dioxide fluxes measurements in a highly vegetated suburban area, Atmos. Environ., 45, 896–905, 2011.

Falge, E., Baldocchi, D., Olson, R., Anthoni, P., Aubinet, M., Bernhofer, C., Burba, G., Ceulemans, R., Clement, R., Dolman, H., Granier, A., Gross, P., Grunwald, T., Hollinger, D., Jensen, N., Katul, G., Keronen, P., Kowalski, A., Lai, C. T., Law, B. E., Meyers, T., Moncrieff, J., Moors, E., Munger, J. W., Pilegaard, K., Rannik, U., Rebmann, C., Suyker, A., Tenhunen, J., Tu, K., Verma, S., Vesala, T., Wilson, K., and Wofsy, S.: Gap filling strategies for defensible annual sums of net ecosystem exchange, Agr. Forest Meteorol., 107, 43–69, 2001.

Foken, T., Göckede, M., Mauder, M., Mahrt, L., Amiro, B., and Munger, W.: Post-field data quality control, in: Handbook of Micrometeorology: A guide for surface flux measurement and analysis, edited by: Lee, X., Massman, W., and Law, B., Kluwer, Dordrecht, 181–208, 2004.

Grimmond, C. S. B., King, T., Cropley, F., Nowak, D., and Souch, C.: Local-scale fluxes of carbon dioxide in urban environments: methodological challenges and results from Chicago, Environ. Pollut., 116, S243–S254, 2002.

Grimmond, C. S. B., Salmond, J. A., Oke, T. R., Offerle, B., and Lemonsu, A.: Flux and turbulence measurements at a densely built-up site in Marseille: Heat, mass (water and carbon dioxide), and momentum, J. Geophys. Res., 109, D24101, doi:10.1029/2004JD004936, 2004.

Helfter, C., Famulari, D., Phillips, G. J., Barlow, J. F., Wood, C. R., Grimmond, C. S. B., and Nemitz, E.: Controls of carbon dioxide concentrations and fluxes above central London, Atmos. Chem. Phys., 11, 1913–1928, doi:10.5194/acp-11-1913-2011, 2011.

Hui, D., Wan S., Su, B., Katul, G., Monson, R., and Luo, Y.: Gap-filling missing data in eddy covariance measurements using multiple imputation (MI) for annual estimations, Agr. Forest Meteorol., 121, 93–111, 2003.

Intergovernmental Panel on Climate Change: IPCC AR4 report, Contribution of working group I to the Fourth Assessment Report of the Intergovermental Panel on Climate Change, Cam-

bridge University Press, Cambridge, United Kingdom and New York, NY, USA, 2007.
Kaimal, J. C. and Finnigan, J. J.: Atmospheric boundary layer flows: Their structure and measurement, Oxford University Press, New York, 289 pp., 1994.
Kalnay, E. and Cai, M.: Impact of urbanization and land-use change on climate, Nature, 423, 528–531, 2003.
Kordowski, K. and Kuttler, W.: Carbon dioxide fluxes over an urban park area, Atmos. Environ., 44, 2722–2730, 2010.
Kormann, R. and Meixner, F. X.: An analytical footprint model for non-neutral stratification, Bound-Lay. Meteorol., 99, 207–224, 2001.
Lee, X., Massman, W., and Law, B.: Handbook of micrometeorology: A guide for surface flux measurement and analysis, Kluwer, Dordrecht, 250 pp., 2004.
Li, Q., Liu, H. Z., Hu, F, Hong, Z. X., and Li, A. G.: The determination of the aero dynamical parameters over urban land surface, Clim. Environ. Res., 8, 443–450, 2003 (in Chinese).
Massman, W. J. and Lee, X.: Eddy covariance flux corrections and uncertainties in long-term studies of carbon and energy exchanges, Agr. Forest Meteorol., 113, 121–144, 2002.
Matese, A., Gioli, B., Vaccari, F. P., Zaldei, A., and Miglietta, F.: Carbon dioxide emissions of the city center of Firenze, Italy: measurement, evaluation, and source partitioning, J. Appl. Meteorol. Climatol., 48, 1940–1947, 2009.
Moriwaki, R. and Kanda, M.: Seasonal and diurnal fluxes of radiation, heat, water vapor, and carbon dioxide over a suburban area, J. Appl. Meteorol., 43, 1700–1710, 2004.
Nemitz, E., Hargreaves, K. J., McDonald, A. G., Dorsey, J. R., and Fowler, D.: Micrometeorological measurements of the urban heat budget and CO_2 emissions on a city scale, Environ. Sci. Technol., 36, 3139–3146, 2002.
Pan, J. and Niu, F.: Annual report on urban development of china, Social Science Literature Publishing, Beijing, China, 2010 (in Chinese).
Pawlak, W., Fortuniak, K., and Siedlecki, M.: Carbon dioxide flux in the centre of Łódź, Poland – analysis of a 2-year eddy covariance measurement data set, Int. J. Climatol., 31, 232–243, 2011.
Satterthwaite, D.: Cities' contribution to global warming: notes on the allocation of greenhouse gas emissions, Environ. Urbanization, 20, 539–549, 2008.
Schotanus, P., Nieuwstadt, F. T. M., and Bruin, H. A. R.: Temperature measurement with a sonic anemometer and its application to heat and moisture fluxes, Bound-Lay. Meteorol., 26, 81–93, 1983.

ACPD
12, 7677–7704, 2012

Eddy covariance measurements of CO_2 and energy fluxes

H. Z. Liu et al.

Song, T. and Wang, Y. S.: Carbon dioxide fluxes from an urban area in Beijing, Atmos. Res., 106, 139–149, 2012.
Stewart, I. D.: Classifying urban climate field sites by "Local Climate Zones", Urban Climate News, 34, 8–11, http://www.urban-climate.org/IAUC034.pdf, 2009.
Velasco, E. and Roth, M.: Cities as Net Sources of CO_2: Review of atmospheric CO_2 exchange in urban environments measured by eddy covariance technique, Geogr. Compass, 4, 1238–1259, 2010.
Velasco, E., Pressley, S., Grivicke, R., Allwine, E., Coons, T., Foster, W., Jobson, B. T., Westberg, H., Ramos, R., Hernández, F., Molina, L. T., and Lamb, B.: Eddy covariance flux measurements of pollutant gases in urban Mexico City, Atmos. Chem. Phys., 9, 7325–7342, doi:10.5194/acp-9-7325-2009, 2009.
Vesala, T., JÄRvi, L., Launiainen, S., Sogachev, A., Rannik, Ü., Mammarella, I., Siivola, E., Keronen, P., Rinne, J, Riikonen, A. N. U., and Nikinmaa, E.: Surface-atmosphere interactions over complex urban terrain in Helsinki, Finland, Tellus, 60B, 188–199, 2008.
Vickers, D. and Mahrt, L.: Quality control and flux sampling problems for tower and aircraft data, J. Atmos. Ocean. Technol., 14, 512–526, 1997.
Vogt, R., Christen, A., Rotach, M. W., Roth, M., and Satyanarayana, A. N. V.: Temporal dynamics of CO_2 fluxes and profiles over a central European city, Theor. Appl. Climatol., 84, 117–126, 2006.
Webb, E. K., Pearman, G. I., and Leuning, R.: Correction of flux measurements for density effects due to heat and water vapour transfer, Q. J. Roy. Meteorol. Soc., 106, 85–100, 1980.
Wood, C. R., Lacser, A., Barlow, J. F., Padhra, A., Belcher, S. E., Nemitz, E., Helfter, C., Famulari, D., and Grimmond, C. S. B.: Turbulent flow at 190m height above London during 2006–2008: A climatology and the applicability of similarity theory, Bound-Lay. Meteorol., 137, 77–96, 2010.

ACPD
12, 7677–7704, 2012

Table 1. Net annual carbon dioxide flux at urban sites around the world.

City	Site	Reference	Annual Total ($kg\ m^{-2}\ y^{-1}$)
Tokyo, Japan	Suburban	Moriwaki and Kanda (2004)	3.52
Cub Hill, Baltimore, USA	Suburban	Crawford et al. (2011)	0.36
Melbourne, Australia	Urban	Coutts et al. (2007)	2.32
London, UK	Urban	Helfter et al. (2010)	9.67
Mexico City, Mexico	Urban	Velasco et al. (2009)	3.49
Essen, Germany	Urban	Kordowski and Kuttler (2010)	1.64
Montreal, Canada	Urban	Bergeron and Strachan (2011)	5.45
Łódź, Poland	Urban	Pawlak et al. (2011)	2.95
Beijing, China	Urban	this study	4.90

ACPD
12, 7677–7704, 2012

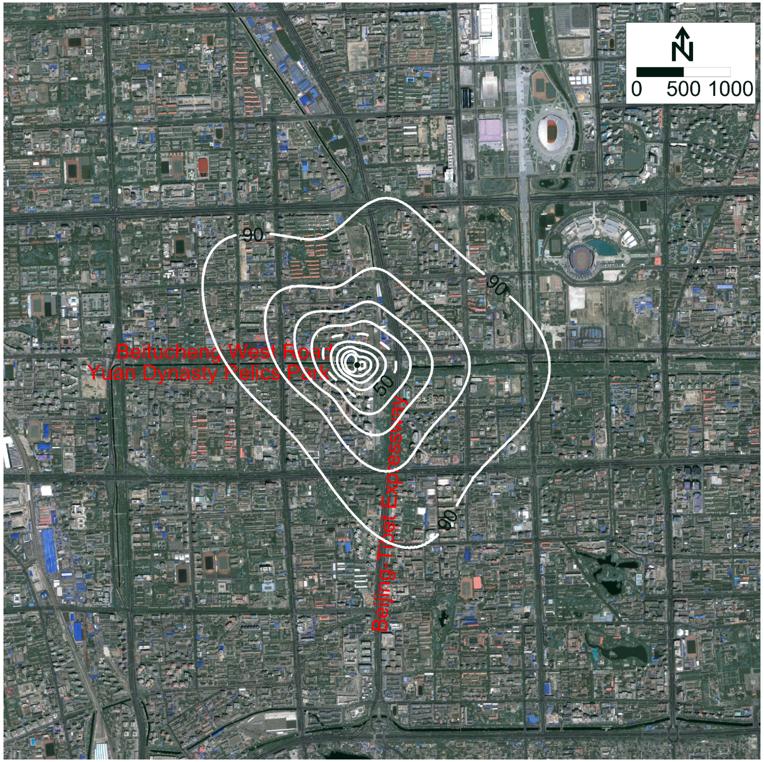

Fig. 1. Satellite photograph of the area around the measurement site taken from Google Earth. Source areas were calculated using the footprint model by Korman and Meixner (2001) from all half-hour data in 2006–2009. White contours represent the percentage of the accumulated flux within the contour. The 50 % contour is marked by a dotted line. The black dot indicates the location of the tower.

ACPD
12, 7677–7704, 2012

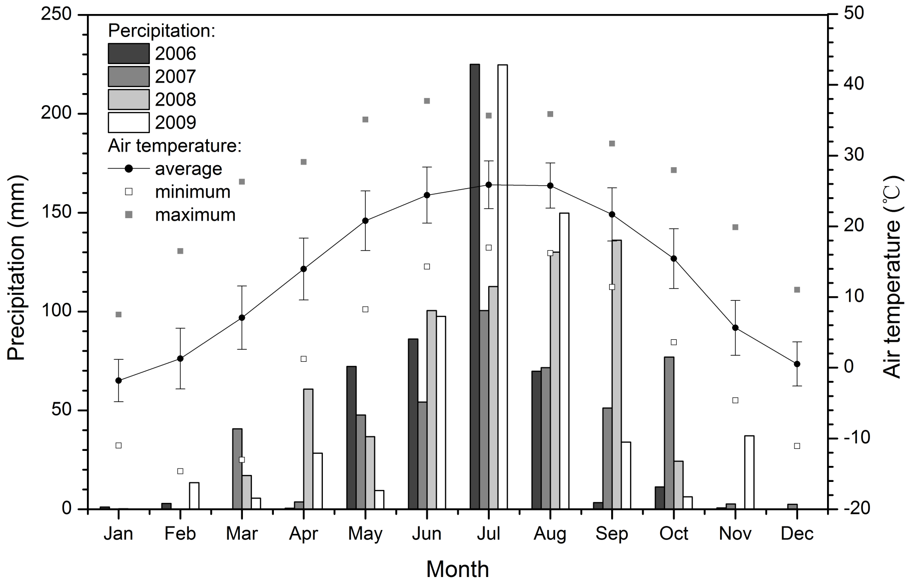

Fig. 2. Monthly precipitation for each study year separately and monthly air temperature for the whole measurement period measured at Caoyang weather station.

ACPD
12, 7677–7704, 2012

Eddy covariance measurements of CO_2 and energy fluxes

H. Z. Liu et al.

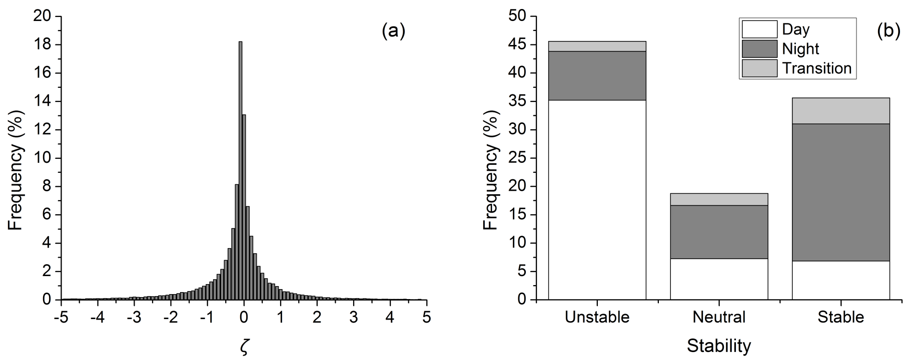

Fig. 3. Frequency histogram of atmospheric stability during the whole measurement period **(a)** and categorized by the time of day **(b)**. Transition period was defined by two hours centered on sunrise/sunset.

ACPD
12, 7677–7704, 2012

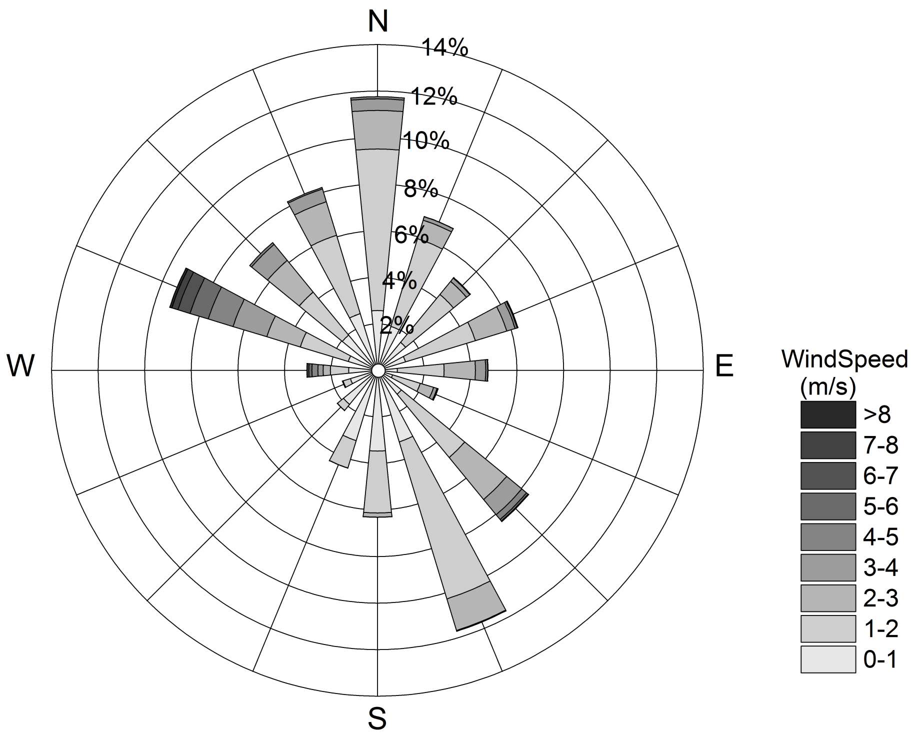

Fig. 4. The wind frequency distribution at 47 m derived from all available data from 2006 to 2009.

ACPD
12, 7677–7704, 2012

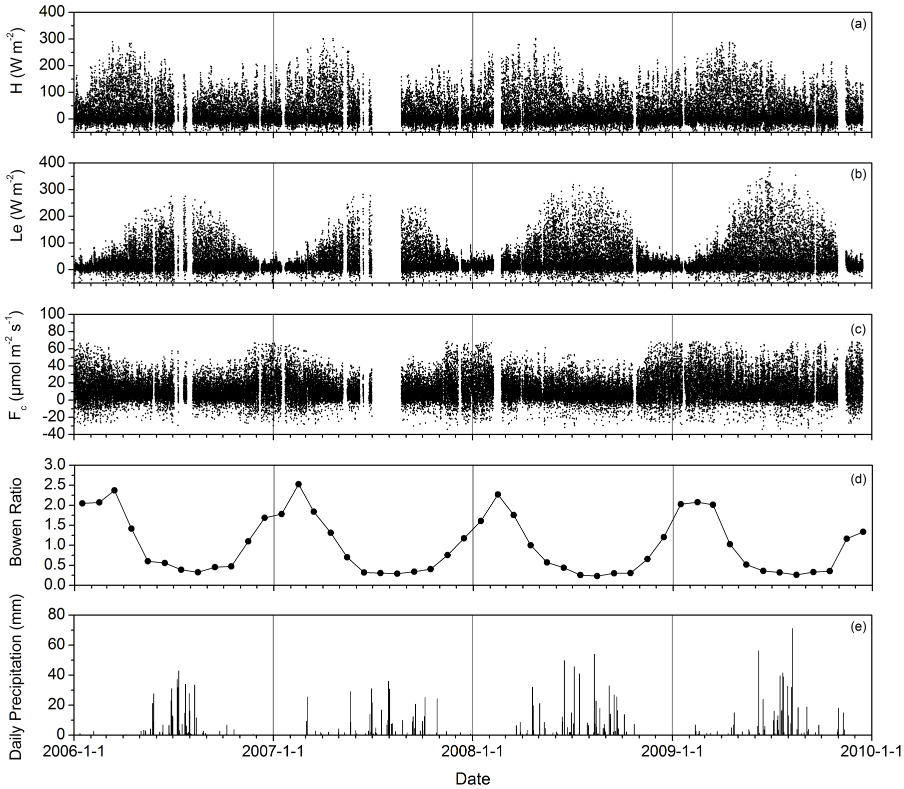

Fig. 5. The time series of sensible heat flux (H) **(a)**, latent heat flux (Le) **(b)**, carbon dioxide flux (F_c) **(c)** at 30 min interval, monthly Bowen ratio **(d)**, and daily total precipitation **(e)** during the study period.

ACPD
12, 7677–7704, 2012

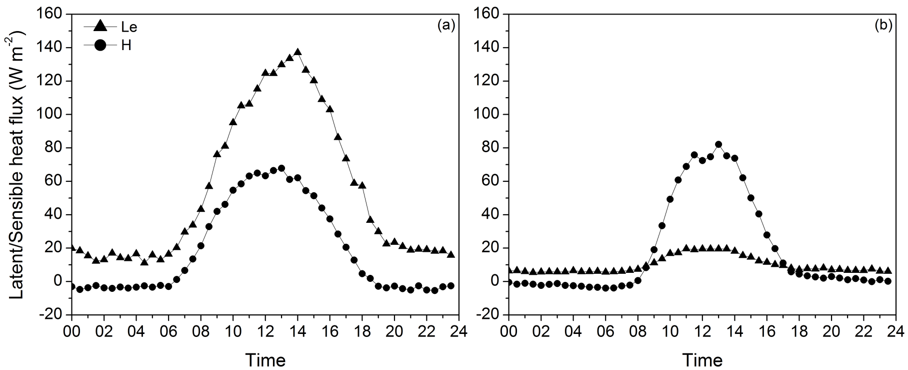

Fig. 6. Average diurnal pattern of latent heat flux (Le) and sensible heat flux (*H*) in summer (JJA, **a**) and winter (DJF, **b**).

ACPD
12, 7677–7704, 2012

Eddy covariance measurements of CO_2 and energy fluxes

H. Z. Liu et al.

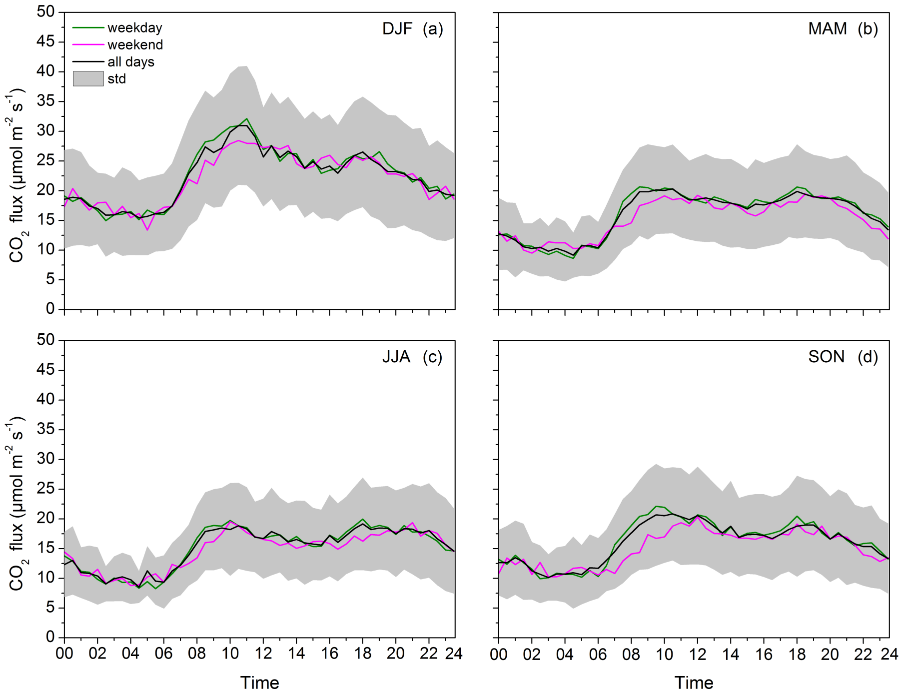

Fig. 7. Average diurnal pattern of F_c for all days, weekdays and weekends separately in DJF **(a)**, MAM **(b)**, JJA **(c)** and SON **(d)** during the study period. The light gray shaded area represents one standard deviation from the mean.

ACPD
12, 7677–7704, 2012

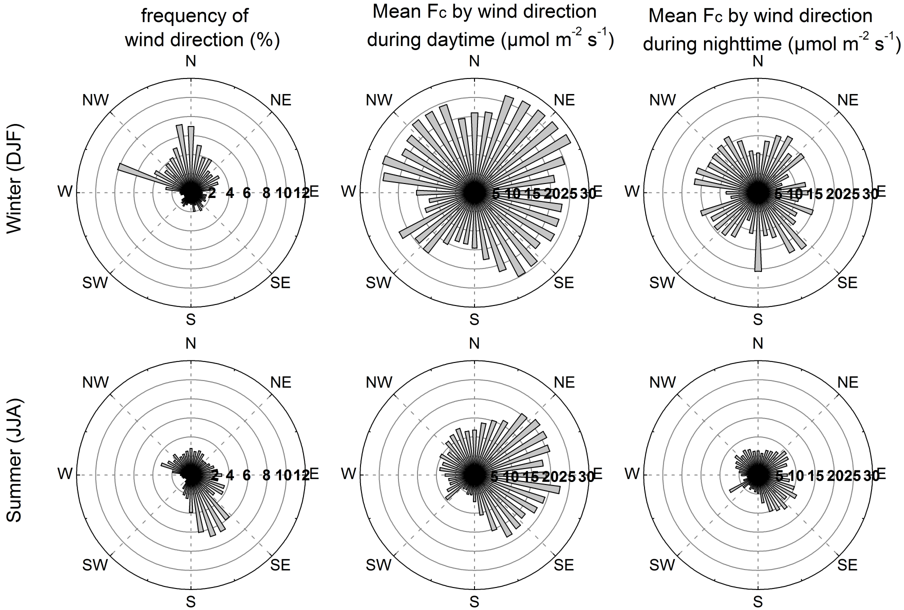

Fig. 8. Wind direction frequency, mean F_c by wind direction during daytime (06:00 a.m.–10:00 p.m.) and nighttime (10:00 p.m.–06:00 a.m.) calculated at 10° intervals from all available data during the study period.

ACPD
12, 7677–7704, 2012

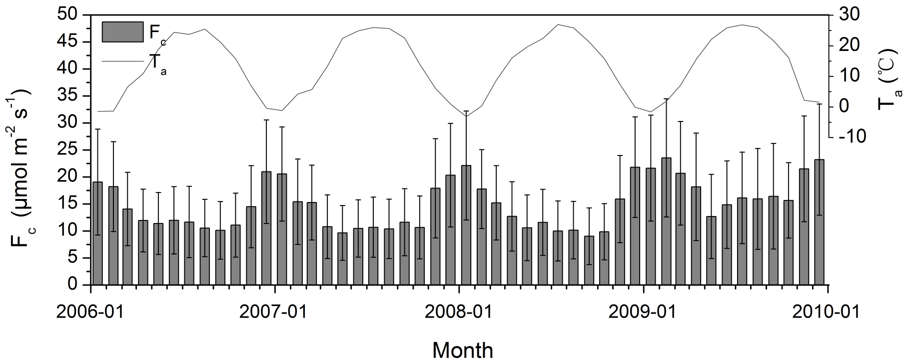

Fig. 9. Monthly average F_c calculated from non-gap-filled dataset and monthly average air temperature (T_a).

ACPD
12, 7677–7704, 2012

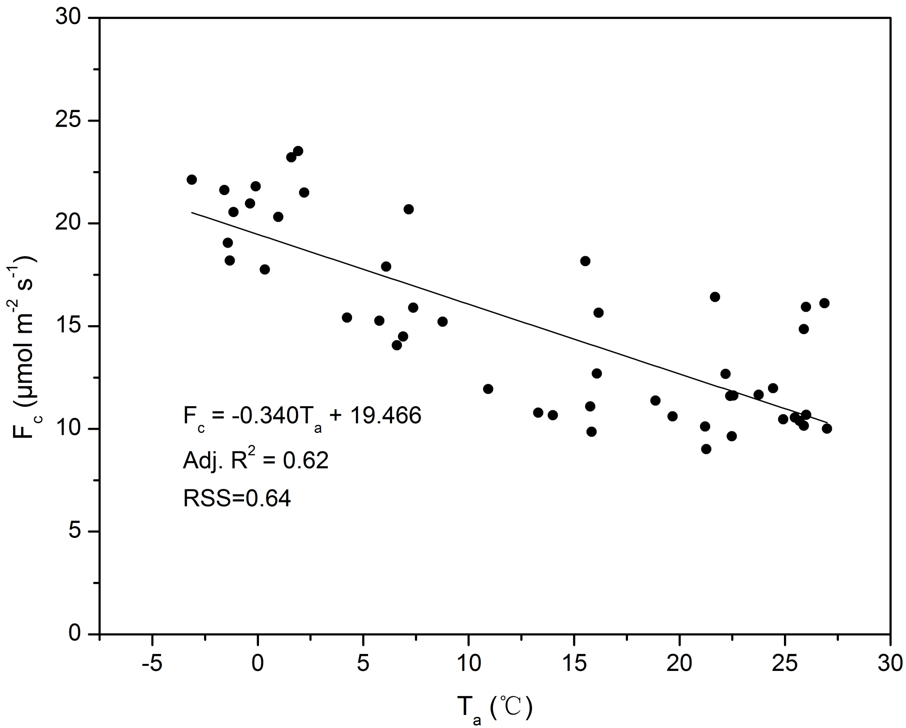

Fig. 10. The relationship between monthly average F_c and air temperature (T_a).

ACPD
12, 7677–7704, 2012